

Thermochemical Relaxation Through Collisions and Radiation

S. Kanne,* H.-H. Frühauf,[†] and E. W. Messerschmid[‡]
University of Stuttgart, 70550 Stuttgart, Germany

A consistent thermochemical relaxation model is presented to calculate high enthalpy flows in a wide velocity and density range. It is based on the coupled vibration–chemistry–vibration model. All types of internal energy, vibrational, rotational, and electronic energy are taken into account. The reaction rate modeling is calibrated using quasi-classical trajectory calculations for dissociation and exchange reactions. The electronic excitation is calculated using quasi-steady-state theory. Radiation is computed using a Monte Carlo method. To couple the flowfield solver and the radiation transport code, the radiative source terms can be implemented into the flowfield solver. Recalculation of the bow shock ultraviolet and FIRE flight experiments show good agreement with measurements.

Nomenclature

A	=	activation energy, J/mol
D	=	dissociation energy, J/mol
J	=	rotational quantum number
k	=	reaction rate, $\text{cm}^3/(\text{mol} \cdot \text{s})$
P	=	proportionality factor, $\text{cm}^3/(\text{mol} \cdot \text{s})$
R	=	gas constant, $8.314 \text{ J}/(\text{mol} \cdot \text{K})$
T	=	temperature, K
U	=	coupled vibration–chemistry–vibration (CVCV) model parameter, K
v	=	vibrational quantum number
α	=	CVCV model parameter
δ	=	linear dependency of the dissociation and activation energy
ε_v	=	vibrational energy, J/mol
λ	=	mean free path, m

Subscripts

A	=	activation energy
D	=	dissociation energy
0	=	ground level

Introduction

FOR the prediction of the heat load at the surface of a reentry vehicle, the state of the plasma has to be known in detail. The kinetic energy of the flow is converted into translational energy of the plasma particles across the bow shock. This energy is then further converted through collisional and radiative processes in the so-called relaxation zone behind the bow shock. The collisional processes can be divided into reactive and nonreactive collisions. In reactive collisions the translational and the internal energies of the atoms and molecules, such as vibrational, rotational, and electronic excitation energy, are converted into chemical enthalpy, whereas in nonreactive collisions, energy is exchanged between the different types of energy.

If the electrons in the shell of an atom or a molecule are at a higher energy level than the ground level, energy can be emitted as photons. This energy can either leave the plasma sheet around the reentry vehicle, it can reach the surface of the vehicle and increase the total heat flux at the wall, or it can be re-absorbed by the plasma at a different location.

Because of the fast energy transfer across the bow shock, the plasma does not necessarily reach the state of thermal or chemical

equilibrium; that is, the distribution of the different energies cannot be described by a single temperature, and the chemical composition cannot be described by the chemical equilibrium constants. However, for a wide range of relevant flows, it is possible to describe each type of energy with a separate temperature, that is, the vibrational and rotational energy. This approach is called multitemperature modeling. It is indispensable for two- or three-dimensional flow calculations to reduce the number of equations to be solved and, hence, to reduce the computation time needed.

Based on the coupled vibration–chemistry–vibration (CVCV) model,¹ a relaxation model is proposed that describes the thermal and chemical relaxation in a wide velocity and density range. Because different processes can take place at different locations of the flow, all energies and species of interest have to be taken into account, that is, including the rotational and electronic energies.² In addition, the electronic excitation is described by quasi-steady-state theory.³ The models were implemented into the URANUS code.⁴ This code considers 11 species and 6 temperatures. Based on the solutions of the flow solver and the electronic excitation, the radiative cooling of the plasma and the radiative heat flux can be calculated with the radiation transport code HERTA.⁵ For large velocities it may be necessary to couple both codes by implementing the radiative source terms into the flow solver due to strong local reabsorption in the plasma.

Internal Energies

Translational Energy

Across the bow shock, the kinetic energy is rapidly transferred into the translational energy of the plasma atoms and molecules. It can be described by a Maxwell distribution for practically all types of continuum flows.

Rotational Energy

Usually rotational energy is assumed always to be in thermal equilibrium with the translational energy due to the narrow energy gap between the different levels. For flows with a very low density, for example, during reentry at high altitudes, this assumption is no longer valid. Although the rotational energy can still be described by a separate temperature, this temperature can strongly differ from the translational temperature. Because of the strong coupling between translational and rotational energy, it is sufficient to consider only the energy transfer between translational and rotational energy, which can be modeled by a Landau–Teller approach (see Ref. 6).

Even if the rotational energy is in thermal equilibrium, its contribution to chemical reactions has to be taken into account for the calculation of reaction rates in a thermal nonequilibrium environment. This will be described later.

Received 13 October 1999; revision received 28 February 2000; accepted for publication 29 February 2000. Copyright © 2000 by the American Institute of Aeronautics and Astronautics, Inc. All rights reserved.

*Research Scientist, Institut für Raumfahrtssysteme. Member AIAA.

[†]Senior Scientist, Institut für Raumfahrtssysteme. Member AIAA.

[‡]Professor, Institut für Raumfahrtssysteme. Member AIAA.

Vibrational Energy

Because of the larger gap between the energy levels, the excitation of the vibrational energy takes much longer than the rotational excitation. Hence, thermal nonequilibrium between translational and vibrational energy is much more likely. The most important energy exchange mechanisms are the exchange between the vibrational energy of the molecule and the translational energy or the vibrational energy of the collisional partner.⁴

Like the rotational energy, vibrational energy contributes to the energy necessary for a reaction to take place. Hence, the vibrational nonequilibrium has to be taken into account for the calculation of chemical reaction rates. Furthermore the vibrational excitation itself is strongly influenced by chemical reactions.

Electronic Excitation Energy

For most flow cases of interest electronic excitation cannot be described by a Boltzmann distribution due to the huge energy gap between ground and excited levels. A more general approach to describe the electronic excitation is to use the quasi-steady-state (QSS) theory.³ Usually electronic excitation occurs by collisions with free electrons. For flows that are hardly ionized, collisions with other atoms and molecules must be also be taken into account. Such an extension to the QSS-model of Park has been proposed by Levin et al.⁷

Besides the energy transfer due to collisions, excited electrons in the shell of the atoms or molecules can emit energy by radiation. To calculate the cooling of the plasma due to radiation and its contribution to the total heat flux at the surface of the reentry vehicle, the radiation transport equation has to be solved. This will be described in more detail later.

Multitemperature Reaction Rates

The CVCV-model was developed by using the concepts of Marrone and Treanor⁸ and by extending their dissociation CVDV modeling to exchange and associative ionization reactions. Later, the influence of rotational energy was included in the model.⁹

The model is based on state-selective reaction rates. The assumption is made that the vibrational energy contributing to overcome the activation barrier is limited by the parameter α to a certain fraction of the activation energy αA . This assumption was made to assure that a minimum fraction of the activation energy comes from the translational energy of the reactants. Therefore, two state-selective reaction rates are given that are different in the second exponential term: Equation (1) if the vibrational energy is lower than this limit and Eq. (2) for higher excited molecules:

$$k(v, J) = P \cdot \exp\{-[D(J) - \varepsilon_v(v)]/\mathcal{R}U\} \times \exp\{-[A(J) - \varepsilon_v(v)]/\mathcal{R}T\}, \quad \varepsilon_v(v) \leq \alpha A(J) \quad (1)$$

$$k(v, J) = P \cdot \exp\{-[D(J) - \varepsilon_v(v)]/\mathcal{R}U\} \times \exp\{-[(1 - \alpha)A(J)]/\mathcal{R}T\}, \quad \varepsilon_v(v) > \alpha A(J) \quad (2)$$

where $\varepsilon_v(v)$ is the molar vibrational energy, $A(J)$ is the molar activation energy, and $D(J)$ is the molar dissociation energy of the molecule in the vibrational ground state depending on the rotational quantum number. P is a proportionality factor that assures that reaction rates are equal to equilibrium rates in case of thermal equilibrium. U describes the preferential reactivity of vibrationally highly excited molecules. D and A are assumed to be linearly dependent on the rotational energy $\varepsilon_r(J)$:

$$D(J) = D_0 - \delta_D \cdot \varepsilon_r(J) \quad (3)$$

$$A(J) = A_0 - \delta_A \cdot \varepsilon_r(J) \quad (4)$$

with $\delta_D = 0.8$ and $\delta_A = 0$ for exchange or $\delta_A = 0.8$ for dissociation reactions.⁹

According to a comparison with a state-selective postshock relaxation computation of Warnatz et al.,¹⁰ we set the two model parameters U and α to be independent of the translational temperature

for all reaction rates ($U = D_0/5$, $\alpha = 0.8$). For dissociation, this could be confirmed by a comparison with another model proposed by Macheret et al.¹¹ For exchange reactions, the model parameters were set to the same values as a first choice. However, these assumptions could not yet be maintained.

By the summing of the state-selective reaction rates over all rotational-vibrational levels weighted by a Boltzmann distribution function, an analytical expression for the overall reaction rates can be obtained. In addition to these rates, the average vibrational and rotational energies gained or removed in chemical reactions are consistently modeled from the state-selective rates. Therefore, both the influence of vibrational energy on reaction rates and the influence of chemical reactions on the average internal energy content of the molecules are taken into account. This is a major advantage over other reaction rate models that treat this influence inconsistently or even neglect this effect.

For further details about the CVCV model see Ref. 1.

Calibration of the CVCV Model

Quasi-Classical Trajectory Method

The quasi-classical trajectory method (QCT) is widely used for modeling of molecular reactions dynamics. It is based on the computation of a large number of trajectories of two particles. The collisions are treated with classical mechanics based on a potential energy surface for the reaction. The trajectory calculation scheme can be seen in Fig. 1. By averaging over the different trajectory parameters, such as velocity and the angle between the particles, we can obtain state-selective reaction rates.

The calculations performed with this method are more effective for large collisional energies and heavy particles. With regard to the translational motion, the de Broglie wavelength should be small enough so that there is no essential change of the potential energy surface within this distance.

Parameter Adjustment

These quasi-classical rates can now be used to verify and adjust the modeling of the state-selective rates of the CVCV model.

Dissociation Reactions

For dissociation reactions, U was initially set to be $D_0/5$, whereas α was assumed to be 0.8. These values were found from a comparison with state-selective rates given by Warnatz et al.¹⁰ Additional comparison with the reaction rate model proposed by Macheret et al.¹¹ confirmed these model parameters for dissociation reactions. Like the extended CVCV model, the model of Macheret et al. also contains a term accounting for the influence of the rotational energy. Both models predict about the same effect of rotational energy.¹¹

In 1986 Levitsky published state-selective reaction rates for various types of reactions (see Ref. 12). He solved the appropriate dynamic model by the method of classical trajectories. Good agreement between these data and the CVCV model can be achieved for $U = D_0/6$ and $\alpha = 0.8$ for O_2 dissociation and $U = D_0/6$ and $\alpha = 0.9$ for N_2 dissociation (see Fig. 2).

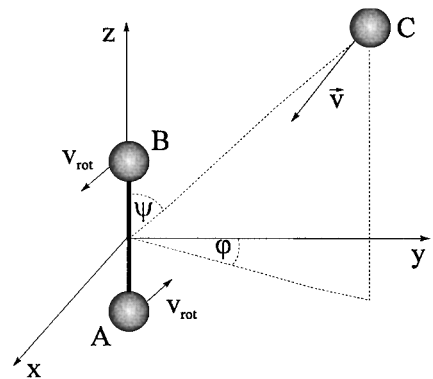


Fig. 1 Trajectory calculation scheme.

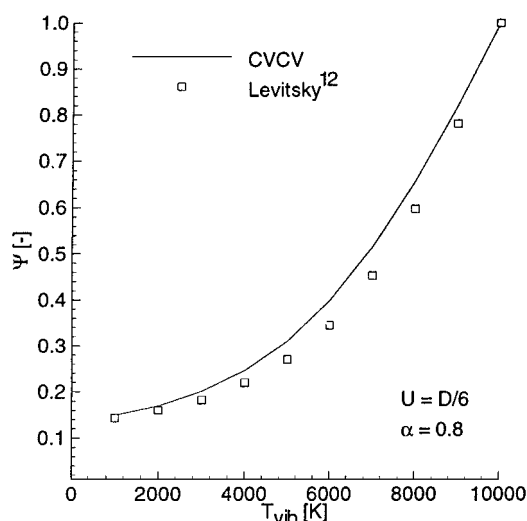


Fig. 2 Nonequilibrium factor for the dissociation of O_2 at $T = 10,000$ K.

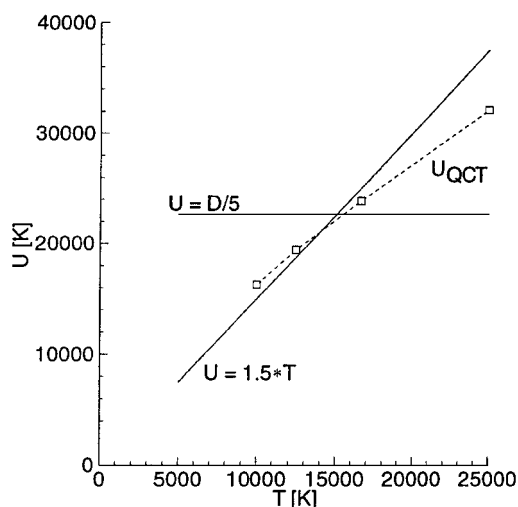


Fig. 3 Dependence of parameter U on translational temperature T .

Exchange Reactions

For air plasmas the most important exchange reactions are the two Zeldovich reactions that determine the production of NO: 1) $NO + O \leftrightarrow N + O_2$ and 2) $N_2 + O \leftrightarrow NO + N$. These rates have been studied by the QCT method in the past in detail, for example, by M. Pogobekyan (Moscow University, private communication) and Bose and Candler.¹³ For the second reaction, a comparison with the calculations of Pogobekyan (private communication) revealed a dependence of U from the translational temperature (Fig. 3). Through the linear approximation $U = 1.5 \cdot T$, a good representation of the QCT results can be achieved for the second reaction.

This temperature dependence indicates that the preferential reactivity of the highly excited molecules diminishes for higher translational temperatures. A possible explanation for this finding is that generally at high temperatures sufficient translational energy is available to overcome the activation barrier. Hence, other energy modes become less important with increasing translational temperature.

Using the preceding approximation for U , we calibrated α to be 0.1 to obtain the best possible agreement between quasi-classical and CVCV-model rates. This means a rather small influence of the vibrational energy on the activation energy for the second Zeldovich reaction. For this type of reaction not only the energy in the collision but also the geometry of the collision, for example, the relative position of the collisional partners, is important. A weak influence of

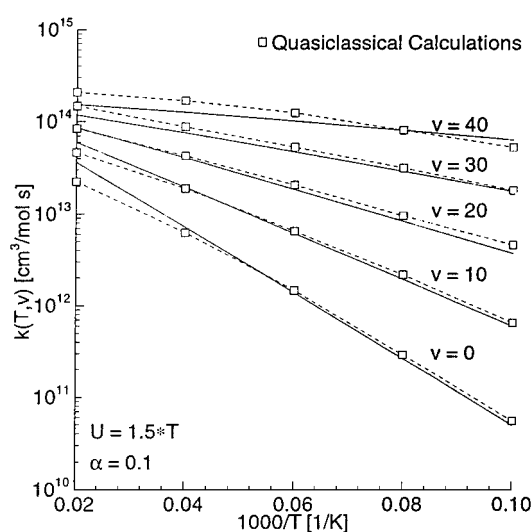


Fig. 4 Comparison of QCT calculations of Pogobekyan (private communication) with the CVCV model ($J = 0$).

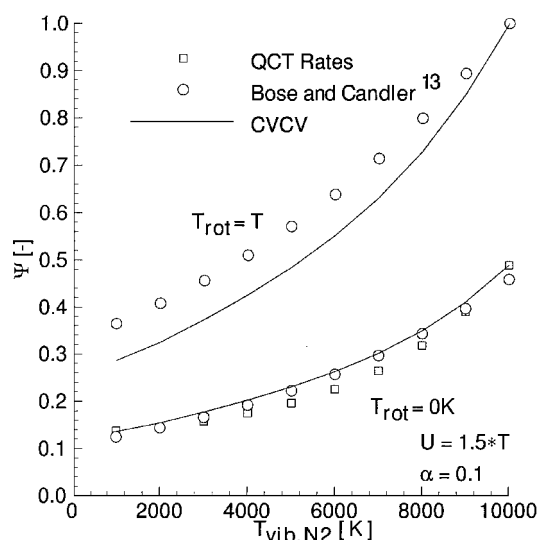


Fig. 5 Nonequilibrium factor for $T = 10,000$ K.

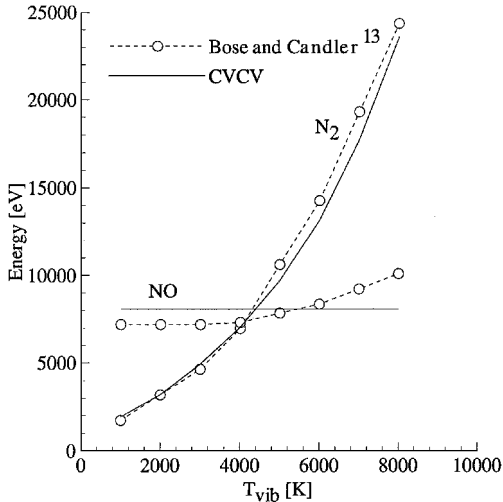
the vibrational energy can, therefore, be considered to be reasonable. Vibrational energy was, hence, found to be much less effective in an exchange compared with a dissociation reaction, where α is set to be about 0.8.

In Fig. 4, rates of the adjusted CVCV model are compared with the quasi-classical rates for the second Zeldovich reaction. A good agreement was achieved across the whole temperature range. The rates were then also compared with rates obtained by Bose and Candler¹³ for this reaction in Fig. 5. Very good agreement was found for both vibrational and rotational nonequilibrium. Especially, the QCT rates of Pogobekyan (private communication) and the rates published by Bose and Candler¹³ show excellent agreement.

In addition to the reaction rates, the average internal energies removed or gained in a reaction are needed for a physically consistent modeling of thermochemical nonequilibrium. In the CVCV model the average internal energy of the product molecule is assumed to be independent of the internal energy of the reactant molecule. Given the principle of detailed balancing, the average energy of the product molecule is set equal to the average energy with which it is removed in the reverse reaction if the reaction is in thermal equilibrium. The best agreement with the data of Bose and Candler¹³ could be achieved if the reverse reaction is assumed to be vibrationally non-preferential ($U \rightarrow \infty$). Because there is nearly no activation energy in this reaction, this assumption seems to be physically reasonable.

Table 1 Comparison of original and adapted CVCV model parameters

Reaction	Original		Adapted	
	U	α	U	α
$N_2 + M \rightarrow N + N + M$	$D_0/5$	0.8	$D_0/6$	0.9
$O_2 + M \rightarrow O + O + M$	$D_0/5$	0.8	$D_0/6$	0.8
$NO + M \rightarrow N + O + M$	$D_0/5$	0.8	$D_0/5$	0.8
$NO + O \rightarrow N + O_2$	$D_0/5$	0.8	$1.5 \cdot T$	0.25
$O_2 + N \rightarrow NO + O$	$D_0/5$	0.8	$12,500 \text{ K} + 2 \cdot T$	0.1
$N_2 + O \rightarrow NO + N$	$D_0/5$	0.8	$1.5 \cdot T$	0.1
$NO + N \rightarrow N_2 + O$	$D_0/5$	0.8	∞	0.1
All other	$D_0/5$	0.8	$D_0/5$	0.8

**Fig. 6** Average vibrational energies removed from N_2 and gained by NO molecules in the second Zeldovich reaction at $T = 8000 \text{ K}$.

In Fig. 6 the average energies of the initial and the product molecule are compared with results of Bose and Candler¹³ for a translational temperature of 8000 K. Excellent agreement was found. Especially the assumption that the average energy of the product molecule NO is independent of the vibrational energy of the initial molecule N_2 is validated.

The parameters of the CVCV model were also adapted for the first Zeldovich reaction using the QCT calculations of Bose and Candler.¹³ The adapted model parameters for the dissociation and exchange reactions are given in Table 1 together with the parameters of the CVCV model that were originally chosen by Knab et al.¹

Radiation

To analyze optical experiments conducted during reentry, the radiation of the plasma must be calculated. For this purpose the plasma radiation database PARADE,¹⁴ developed in the framework of an ESA/European Space Research and Technology Center technical research project, has been extended to allow for the calculation of the radiation from all molecules that are important in air plasma radiation. As radiation mechanisms, continuum, atomic line, and molecular radiation are included. For the atomic line radiation, the shape of the lines is assumed to be a Voigt profile. The broadening of these lines consists of Doppler, Stark, Van der Waals, resonance, natural, and phase broadening. The molecular radiation is taken from NEQAIR.

The radiative properties of the flow can only be computed if the number densities of the excited states are known beforehand. The complex calculation of nonequilibrium excitation is performed using the QSS approximation from NEQAIR. For most cases, electronic excitation is dominated by collisions with free electrons. However, for plasmas that are weakly ionized, electronic excitation due to heavy particle collisions must be taken into account. This is done using the model proposed by Levin et al.⁷

Results for the emission and absorption coefficient can be highly dependent on the spectral resolution of the database. Therefore, a new approach is made for the wavelength discretization of the absorption and emission spectra. This new discretization technique was developed at the University of Tennessee Space Institute and the Space Systems Institute of the University of Stuttgart. It is designed to require less memory than an equal frequency or wavelength discretization technique and to be fully self-adaptive.

By the use of a self-adaptive technique, spacing between adjacent points becomes closer for regions of high emission and wider for those of low emission. This gives appropriate resolutions for each part of the spectrum. The method is based on a simplified precalculation of the atomic spectra, that is, the distribution of the atomic emission coefficient over a specific wavelength range. The main principle of the discretization process is to divide the spectral range into a number of subranges based on the precalculation so that the energy emitted by atomic radiation is almost equal for each subrange. Only the complex structure of the molecular radiation is still treated in the usual way.

Because emitted radiation can be reabsorbed by the fluid, its way through the flowfield must be tracked to compute correctly the radiative heat flux at the body surface and the radiative source terms for the flowfield solver. Here, a Monte Carlo method is used for the calculation of the gas radiation transport. The entire code system HERTA is able to compute reabsorptive radiation fields in chemical and thermal nonequilibrium in a fully spectral manner for generic axisymmetric geometries for either convex or nonconvex body shapes.

The modeling of radiation energy transport can be briefly characterized as follows: The basic physical phenomena are represented as random processes and controlled by means of computer-generated random numbers. The radiation field is spatially discretized by means of a calculation grid by distinct volume elements. The boundary conditions are implemented. A number of radiation bundles depending on the local thermodynamic parameters, the pressure, the temperatures, and the chemical composition is emitted out of each grid cell with stochastically determined direction and wavelength. The respective stochastic distribution functions have to represent the true physical situation for a large number of radiation bundles. Each single bundle, representing a number of photons, is then tracked on its way through the calculation domain, accounting for its absorption.

The solution quantities are divergence of the radiative flux $\nabla \cdot \mathbf{q}_r$, as necessary for coupling with a flowfield solver and the radiative fluxes across the boundaries of the computational domain. The latter quantity is sampled on each boundary surface element spectrally resolved. All impinging bundles are considered. The total radiative flux is obtained after a spectral integration. Thus, a space covering half a solid angle is observed, as is necessary to obtain the overall radiative flux on the surface elements.

However, typical radiation experiments usually observe only a narrow cone element as given by the experimental setup and focusing optics. Therefore, a procedure was implemented into the code to simulate these experiments. Only bundles impinging on the surface within a cone of the user-specified half opening angle around the surface normal is taken into account for the simulation of optical experiments.

Test Cases

Bow Shock Ultraviolet Experiment II

In 1990 and 1991 two sounding rocket experiments were conducted: Bow Shock Ultraviolet Experiments (BSUV) I and II.^{15,16} During both flights, various optical measurements were carried out to gain detailed information about the state of the plasma in front of the entry vehicle. In these measurements, the NO molecular band radiation was found to be very strong. Up to now, most reaction rate models did not consistently model the average vibrational energies removed or gained in reactions. Hence, molecules were not expected to be created vibrationally highly excited, and the strong radiation signals could not be recalculated using these conventional rate models.

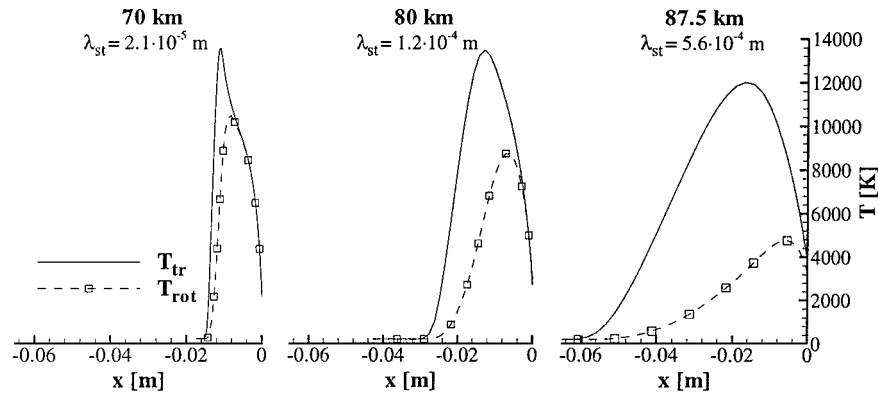


Fig. 7 Rotational temperature along the stagnation streamline: BSUV II.

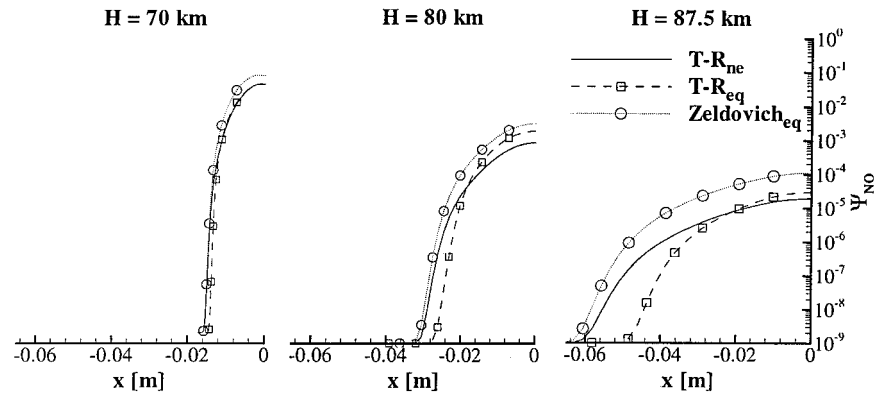


Fig. 8 NO mole fraction along the stagnation streamline: BSUV II.

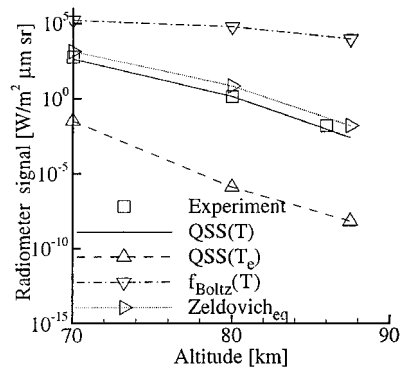


Fig. 9 Radiometer signal at the stagnation point: BSUV II.

For this reason Bose and Candler¹³ have carried out QCT calculations to understand the kinetic processes in the plasma better. These results have been implemented into the CVCV model as described earlier. Through the use of axisymmetric flow solver URANUS and the radiation transport code HERTA, the BSUV experiments were calculated to validate the modeling of the processes in the plasma. The mesh for the flow solver was resolved up to the scale of the mean free path near the surface of the vehicle to assure a numerically accurate solution. In the case of the Monte Carlo process used in HERTA, the number of bundles used was increased until no change in result occurred. The results for the second BSUV experiment will be presented in the following. As can be seen in Fig. 7 there is a strong thermal nonequilibrium between the rotational and the translational temperature for high altitudes.

If this nonequilibrium were neglected, the dissociation rates would be overestimated due to the contribution of the rotational energy. This leads to an earlier production of NO, as can be seen from Fig. 8, because atomic oxygen is necessary for the Zeldovich reaction to take place. If in addition the vibrational nonequilibrium

is neglected and hence a single-temperature reaction rate model is used ($Zeldovich_{eq}$), the NO production is overestimated up to a factor of five. As a consequence, the radiation signal would be also a factor of five higher than the measurements (Fig. 9). However, as can be seen, the accurate modeling of the electronic excitation is much more important. If either a Boltzmann distribution is assumed for the excitation, f_{Boltz} , or if the collisions with heavy particles are neglected, $QSS(T_e)$, the predicted radiation signal would differ in order of magnitudes from the measured signal.

If the NO production is modeled correctly, the predicted amount of atomic oxygen in the flow must also be correct. In Fig. 10 the measured O radiation is compared with the results of the radiation transport calculation. As can be seen, there is also a very good agreement for the oxygen atomic line radiation.

FIRE II

In 1964 a reentry experiment, FIRE,¹⁷ was conducted in the framework of the Apollo moon program. During the reentry, the

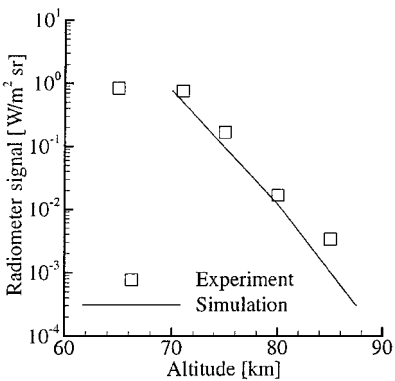


Fig. 10 Atomic oxygen radiation at 130.4 nm.

total and the radiative heat flux on the surface of the vehicle were measured using a calorimeter and radiometer, respectively. At an altitude of 67 km, the velocity was 11.25 km/s. At such a high velocity, radiation cooling and radiative surface heat flux become important. Contrary to the BSUV flight experiments, the flow around the FIRE vehicle is strongly influenced by ionization. The population of the highly excited electronic energy levels, which determine the ionization rates, might even deviate from a Boltzmann distribution. To study the capability of the reaction rate modeling presented earlier for this type of flow, and to study the influence of the electronic excitation on the ionization of the flow, this point of the flight trajectory was recalculated. The temperatures and the mole fractions calculated along the stagnation streamline are given in Figs. 11 and 12, respectively.

Using the QSS theory, we calculate the distribution of the electronic excitation energy. It is shown in Fig. 13 at different positions

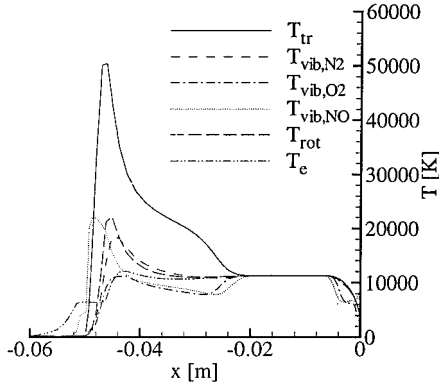


Fig. 11 Temperatures along the stagnation streamline: FIRE, $H = 67$ km.

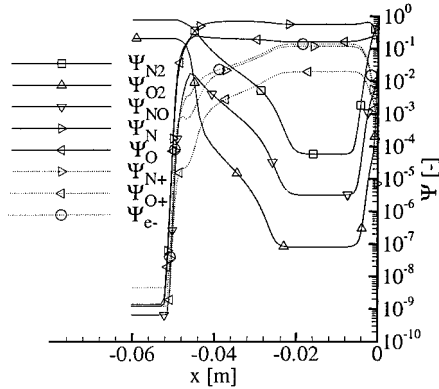


Fig. 12 Mole fractions along the stagnation streamline: FIRE, $H = 67$ km.

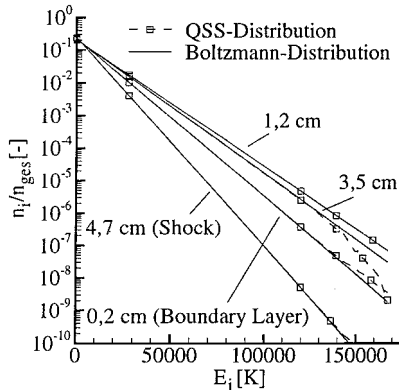


Fig. 13 Number densities of the excited levels for atomic nitrogen at different positions of the stagnation streamline: FIRE, $H = 67$ km.

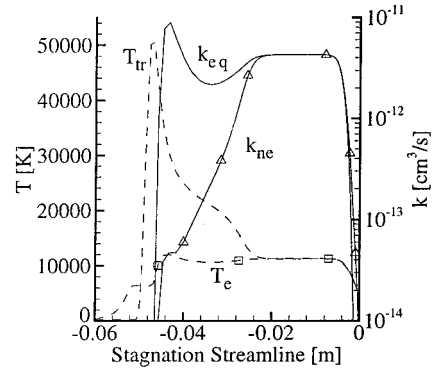


Fig. 14 Ionization rates along the stagnation streamline: FIRE, $H = 67$ km.

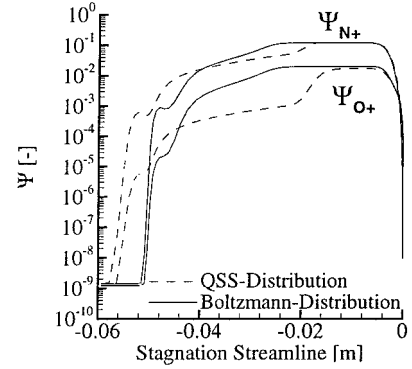


Fig. 15 Mole fractions of ionized oxygen and nitrogen along the stagnation streamline: FIRE, $H = 67$ km.

on the stagnation streamline. Compared to a Boltzmann distribution, the upper levels are less populated behind the shock, assuming a QSS distribution due to the relaxation process. The opposite holds true for the boundary layer. The distribution of the electronic excitation is then consistently coupled into the flowfield solver, especially for the computation of the atomic ionization rates.

The influence of this nonequilibrium is shown in Fig. 14. Because ionization is dominated by the number densities of the upper levels, reaction rates based on QSS-theory, k_{ne} , are much lower behind the shock. As a consequence of the lower ionization rates, chemical equilibrium is reached later if a QSS distribution of the excited electronic levels is assumed, as shown in Fig. 15.

Although ionization rates are lower in the postshock region assuming a QSS distribution (due to the smaller number densities of highly excited particles), this has no influence on the surface heat flux because chemical and thermal equilibrium is already reached in front of the boundary layer. Because the boundary layer is dominated by recombination, differences in ionization rates are negligible. However, for highly ionized flows without a region of thermochemical equilibrium, the influence of a nonequilibrium distribution of the highly excited electronic levels on ionization and surface heat flux can be much stronger.

For the trajectory point calculated here, the radiative heat flux becomes important. The radiative heat flux is about 15% of the total heat flux. The plasma temperature is lowered due to the radiative cooling leading to a lower temperature at the boundary-layer edge and, hence, to a lower convective heat flux. However, this effect is partly compensated due to the strong reabsorption in the relatively cold boundary layer.

Conclusions

For accurate local simulation of high enthalpy flows, the various physical and chemical processes must be described in detail. The chemical nonequilibrium and the coupling between thermal and chemical nonequilibrium can be described by the CVCV model of Knab et al.,¹ which was extended to account for the contribution of the rotational energy.

Using QCT calculations, we calibrated the model parameters for dissociation and exchange reactions. It was found that vibrational energy is much more effective in dissociation reaction than in exchange reactions. Furthermore, the parameter U , describing the preferential reactivity of highly excited molecules, was found to be dependent on the translational temperature for exchange reactions. For exchange reactions, the preferential reactivity diminishes for higher translational temperatures.

Apart from vibrational nonequilibrium, rotational nonequilibrium becomes important for high altitudes because rotational energy has a strong influence on dissociation reactions. Even in case of equilibrium between translational and rotational temperature, the contribution of the rotational energy must be taken into account for the calculation of reaction rates in case of nonequilibrium between vibrational and translational energies.

Reaction rate models such as the CVCV model can be validated using optical measurements conducted during reentry. Comparison between measurements of the BSUV flight experiments and radiation simulations shows good agreement. Hereby, an accurate modeling of the electronic excitation is crucial. For weakly ionized flows like the BSUV, electronic excitation due to heavy particles as described by the model of Levin et al.⁷ cannot be neglected.

For highly ionized flows like the FIRE II experiment, the radiative cooling of the plasma becomes important, and reabsorption of the radiation must be taken into account. Because of the strong electronic excitation, QSS theory reveals a deviation from the Boltzmann distribution. This leads to lower ionization rates directly behind the shock. However, because of a region of thermal and chemical equilibrium upstream of the boundary layer, this has practically no influence on the surface heat flux.

With this modeling of thermal and chemical nonequilibrium, the URANUS code makes it possible to calculate different types of flows in great detail. All types of energies, which have a significant influence on the flow behavior, such as vibrational, rotational and electronic excitation, are taken into account.

Acknowledgment

This work was supported by the Deutsche Forschungsgemeinschaft.

References

¹Knab, O., Frühauf, H.-H., and Messerschmid, E. W., "Theory and Validation of the Physically Consistent Coupled Vibration-Chemistry-Vibration Model," *Journal of Thermophysics and Heat Transfer*, Vol. 9, No. 2, 1995, pp. 219–226.

²Kanne, S., "Zur thermo-chemischen Relaxation innerer Freiheitsgrade durch Stoß- und Strahlungsprozesse beim Wiedereintritt," Dissertation, Univ. of Stuttgart, Stuttgart, Germany, June 2000.

³Park, C., *Nonequilibrium Hypersonic Aerothermodynamics*, Wiley, New York, 1990, pp. 90–118.

⁴Daiß, A., Schöll, E., Frühauf, H.-H., and Knab, O., "Validation of the URANUS Navier–Stokes Code for High-Temperature Nonequilibrium Flow," AIAA Paper 93-5070, Nov. 1993.

⁵Gogel, T. H., Dupuis, M., and Messerschmid, E. W., "Radiation Transport Calculation in High Enthalpy Environments for Two-Dimensional Axisymmetric Geometries," *Journal of Thermophysics and Heat Transfer*, Vol. 8, No. 4, 1994, pp. 744–750.

⁶Parker, J. G., "Rotational and Vibrational Relaxation in Diatomic Gases," *Physics of Fluids*, Vol. 2, No. 4, 1959, pp. 449–463.

⁷Levin, D. A., Braunstein, M., Candler, G. V., Collins, R. J., and Smith, G. P., "Examination of Theory for Bow Shock Ultraviolet Rocket Experiments, Part II," *Journal of Thermophysics and Heat Transfer*, Vol. 8, No. 3, 1994, pp. 453–459.

⁸Marrone, P. V., and Treanor, C. E., "Chemical Relaxation with Preferential Dissociation from Excited Vibrational Levels," *Physics of Fluids*, Vol. 6, No. 9, 1963, pp. 1215–1221.

⁹Kanne, S., Knab, O., Frühauf, H.-H., and Messerschmid, E. W., "The Influence of Rotational Excitation on Vibration–Chemistry–Vibration Coupling," AIAA Paper 96-1802, June 1996.

¹⁰Warnatz, J., Riedel, U., and Schmidt, R., "Different Levels of Air Dissociation Chemistry and Its Coupling with Flow Models," *Proceedings of the 2nd Joint Europe–U.S. Short Course in Hypersonics*, Birkhäuser, Boston, 1992, pp. 67–103.

¹¹Macheret, S. O., Fridman, A. A., Adamovich, I. V., Rich, J. W., and Treanor, C. E., "Mechanisms of Nonequilibrium Dissociation of Diatomic Molecules," AIAA Paper 94-1884, June 1994.

¹²Sergievskaia, A. L., Kovach, E. A., Losev, S. A., and Kuznetsov, N. M., "Thermal Nonequilibrium Models for Dissociation and Chemical Exchange Reactions at High Temperatures," AIAA Paper 96-1895, June 1996.

¹³Bose, D., and Candler, G. V., "Simulation of Hypersonic Flows Using a Detailed Nitric Oxide Formation Model," *Physics of Fluids*, Vol. 9, No. 4, 1997, pp. 1171–1181.

¹⁴Kanne, S., Gogel, T. H., Dupuis, M., and Messerschmid, E. W., "Simulation of Radiation Experiments on Reentry Vehicles Using the New Radiation Database PARADE," AIAA Paper 97-2562, June 1997.

¹⁵Erdman, P. W., Zipf, C., Espy, P., Howlett, C. L., Levin, D. A., Loda, R., Collins, R. J., and Candler, G. V., "Flight Measurements of Low-Velocity Bow Shock Ultraviolet Radiation," *Journal of Thermophysics and Heat Transfer*, Vol. 7, No. 1, 1993, pp. 37–41.

¹⁶Erdman, P. W., Zipf, C., Espy, P., Howlett, C. L., Levin, D. A., Collins, R. J., and Candler, G. V., "Measurements of Ultraviolet Radiation from a 5-km/s Bow Shock," *Journal of Thermophysics and Heat Transfer*, Vol. 8, No. 3, 1994, pp. 441–446.

¹⁷Cauchon, D. L., "Radiative Heating Results from the FIRE II Flight Experiment at a Reentry Velocity of 11.4 Kilometers per Second," NASA TM X-1402, July 1967.